Implementing quantum gates using the ferromagnetic spin-J XXZ chain with kink boundary conditions

New Journal of Physics
The open-access journal for physics

Implementing quantum gates using the ferromagnetic spin-*J* XXZ chain with kink boundary conditions

Tom Michoel[1], **Jaideep Mulherkar**[2] **and Bruno Nachtergaele**[2,3]

[1] Department of Plant Systems Biology, VIB, Department of Molecular Genetics, Ghent University, Technologiepark 927, B-9052 Gent, Belgium
[2] Department of Mathematics, University of California, Davis, CA 95616-8633, USA
E-mail: bxn@math.ucdavis.edu

New Journal of Physics **12** (2010) 025003 (15pp)
Received 30 April 2009
Published 26 February 2010
Online at http://www.njp.org/
doi:10.1088/1367-2630/12/2/025003

Abstract. We demonstrate an implementation scheme for constructing quantum gates using unitary evolutions of the one-dimensional spin-*J* ferromagnetic XXZ chain. We present numerical results based on simulations of the chain using the time-dependent density matrix renormalization group method and techniques from optimal control theory. Using only a few control parameters, we find that it is possible to implement one- and two-qubit gates on a system of spin-$\frac{3}{2}$ XXZ chains, such as Not, Hadamard, Pi-8, Phase and C-Not, with fidelity levels exceeding 99%.

[3] Author to whom any correspondence should be addressed.

Contents

1. Introduction **2**
2. The model **4**
3. Quantum gates using quantum control **5**
3.1. Single qubit gates 5
3.2. Implementing two-qubit gates 6
3.3. Optimal control 8
4. DMRG simulations for quantum gates **10**
5. Results **11**
Acknowledgments **14**
References **15**

1. Introduction

For quantum computers to become a reality we need to find or build physical systems that faithfully implement the quantum gates used in the algorithms of quantum computation. The basic requirement is that the experimenter has access to two states of a quantum system that can be effectively decoupled from environmental noise for a sufficiently long time, and that transitions between these two states can be controlled to simulate a number of elementary quantum gates (unitary transformations). Systems that have been investigated intensively are atomic levels in ion traps [1, 2], superconducting device physics using Josephson rings [3], nuclear spins [4] (using NMR in suitable molecules) and quantum dots [5]. In this paper, we demonstrate the implementation of quantum gates using one-dimensional spin-J systems. The results are obtained using a computer simulation of these systems.

The Hamiltonian of the XXZ model with kink boundary conditions is given by

$$H_L^{\mathrm{k}}(\Delta^{-1}) = \sum_{\alpha=-L+1}^{L-1} \left[(J^2 - S_\alpha^3 S_{\alpha+1}^3) - \Delta^{-1}(S_\alpha^1 S_{\alpha+1}^1 + S_\alpha^2 S_{\alpha+1}^2) \right] + J\sqrt{1-\Delta^{-2}}(S_{-L+1}^3 - S_L^3), \qquad (1)$$

where S_α^1, S_α^2 and S_α^3 are the spin-J matrices acting on the site α. Apart from the magnitude of the spins, J, the main parameter of the model is the anisotropy $\Delta > 1$ and the limit $\Delta \to \infty$ is referred to as the *Ising limit*. In the case of $J = \frac{1}{2}$ kink boundary conditions were first introduced in [6]. They lead to ground states with a domain wall between down spins on the left portion of the chain and up spins on the right. The third component of the magnetization, S_{tot}^3, is conserved, and there is exactly one ground state for each value of M. Different values of M correspond to different positions of the domain walls, which in one dimension are sometimes referred to as kinks. In [7], Koma *et al* showed that there is a spectral gap above each of the ground states in this model for all values of J. Recently [8] it was shown that for spin values $J \geqslant \frac{3}{2}$ and for sufficiently large value of the anisotropy Δ the low lying spectrum of (1) for each value of M has isolated eigenvalues that persist in the thermodynamic limit.

The presence of isolated eigenvalues is ideal from the point of view of quantum computation. The idea is to use the subspace, denoted by $\mathcal{D}$, of the ground state and the first excited state of the Hamiltonian to encode a qubit. In the absence of noise (coupling to

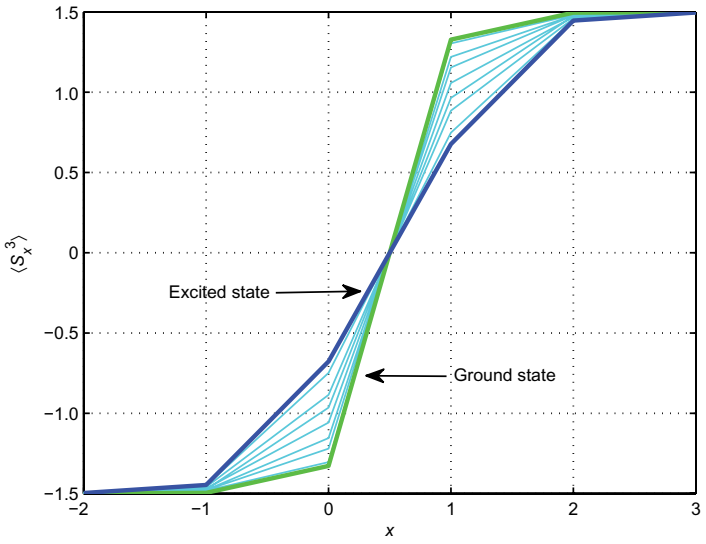

Figure 1. The transitioning of the magnetization profile from the ground to the first excited state using a Not gate. Simulation obtained for a chain of 50 ($L = 25$) sites using DMRG with $\Delta^{-1} = 0.3$ and $M = 0$. The lines in between the ground and excited state profiles represent the profile at intermediate times between $t = 0$ and the gate time $T = 20$.

the environment), states corresponding to eigenvalues have an infinite life time. Generically, when the eigenvalues are embedded in a continuum, arbitrarily small perturbations will turn them into resonances, i.e. states with a finite life time. By using a subspace of states corresponding to isolated eigenvalues, we can expect much larger life times even in the presence of noise. Heuristically, there is an energy barrier protecting the states from decaying. Since the eigenvalues are *not* protected by a topological invariant, it is possible to use local, finite-strength perturbations to control transitions in the system. In principle, such perturbations may be implemented in a suitable solid state setup.

Concretely the idea is to let the system evolve under its own unitary time evolution generated by the Hamiltonian (1) with the addition of a few local control fields. We have two requirements to fulfill: the time evolution should leave the qubit space $\mathcal{D}$ approximately invariant, and the (approximately) unitary matrix describing the dynamics restricted to $\mathcal{D}$ and stopped at a suitable time should coincide with the desired quantum gate.

The control inputs needed to drive the system such that high fidelity gates are obtained are determined using techniques from optimal control theory. The simulation of the time evolution of the chain that is large enough to resemble the properties in the thermodynamic limit is carried out using the density matrix renormalization group (DMRG) algorithm. Figure 1 shows the transition of the magnetic profiles in the z-direction from the ground to the first excited state using the Not gate constructed from a spin-$\frac{3}{2}$ XXZ spin chain of length 50 sites. We also demonstrate the construction of Pi-8, Hadamard and Phase gates that form a set of universal single qubit gates.

In order to have a viable quantum computing scheme one needs to implement at least one two-qubit gate. Here, we have implemented the C-Not gate which, in combination with the one-qubit gates, is known to be universal [9].

Our scheme capitalizes on the kink nature of the excitations of the XXZ Hamiltonian, which are rather sharply localized. We imagine a setup with two parallel chains with the location of the kink lined up in their ground states. The subspace for the two-qubit state space is then $\mathcal{D}_1 \otimes \mathcal{D}_2$, where $\mathcal{D}_1$ represents the space of isolated eigenvalues of the first chain and $\mathcal{D}_2$ for the second chain. A set of three controls localized near the kinks is used to generate the single qubit gates acting on $\mathcal{D}_1$ and $\mathcal{D}_2$ and a C-Not gate on $\mathcal{D}_1 \otimes \mathcal{D}_2$. This scheme produces a universal set of gates necessary for two-qubit computation. It is clear how to generalize this scheme to implement n-qubit computation. Since a universal set of single qubit gates and nearest neighbor C-Not gates are universal for n-qubit computation, this can be achieved by using n parallel chains and controls that are localized and act on neighboring chains only.

In the next section, we describe the model and review some of the past results. Then, in section 3, the optimal control problem to construct the quantum gates is described. Section 4 is devoted to the DMRG algorithm and the specific adaptations to the XXZ spin chain. Finally, in section 5 we present our results based on numerical simulations of the XXZ Hamiltonian using the DMRG algorithm.

2. The model

In this section we describe in detail the spin-J ferromagnetic XXZ model with kink boundary conditions on the one-dimensional lattice $\mathbb{Z}$. The local Hilbert space for a single site α is $\mathcal{H}_\alpha = \mathbb{C}^{2J+1}$ with $J \in \frac{1}{2}\mathbb{N} = \{0, \frac{1}{2}, 1, \frac{3}{2}, 2, \ldots\}$. We consider the Hilbert space for a finite chain on the sites $[-L+1, L] = \{-L+1, -L+2, \ldots, +L\}$. This is $\mathcal{H}_{[-L+1,L]} = \bigotimes_{\alpha=-L+1}^{L} \mathcal{H}_\alpha$. The Hamiltonian of the spin-J XXZ model is given by equation (1). Note that, by a telescoping sum, we can absorb the boundary fields into the local interactions:

$$H_L^{\mathrm{k}}(\Delta^{-1}) = \sum_{\alpha=-L+1}^{L-1} h_{\alpha,\alpha+1}^{\mathrm{k}}(\Delta^{-1}),$$

$$h_{\alpha,\alpha+1}^{\mathrm{k}}(\Delta^{-1}) = J^2 - S_\alpha^3 S_{\alpha+1}^3 - \Delta^{-1}(S_\alpha^1 S_{\alpha+1}^1 + S_\alpha^2 S_{\alpha+1}^2) + J\sqrt{1-\Delta^{-2}}\,(S_\alpha^3 - S_{\alpha+1}^3).$$

The main parameter of the model is the anisotropy $\Delta > 1$ and we get the Ising limit as $\Delta \to \infty$. It is mathematically more convenient to work with the parameter Δ^{-1}, which we then assume is in the interval $[0, 1]$. As we said, $\Delta^{-1} = 0$ is the Ising limit, and $\Delta^{-1} = 1$ is the isotropic XXX Heisenberg model. The Hamiltonian commutes with the total magnetization

$$S_{\mathrm{tot}}^3 = \sum_{\alpha=-L}^{L} S_\alpha^3.$$

As indicated in the introduction, for each $M \in \{-2JL, -2JL+1, \ldots, 2JL\}$, the corresponding sector is defined to be the eigenspace of S_{tot}^3 with eigenvalue M; clearly, these are invariant subspaces for all the Hamiltonians introduced above. These subspaces are called 'sectors'.

It was shown [6, 10, 11, 13, 14] that the kink boundary conditions lead to a family of ground states. It was also shown in [10]–[13] that for each sector there is a unique ground state of $H_L^{\mathrm{k}}(\Delta^{-1})$ with eigenvalue 0. Moreover, this ground state, ψ_M, is given by the following

expression:

$$\psi_M = \sum \bigotimes_{\alpha\in[-L+1,L]} \binom{2J}{J-m_\alpha}^{1/2} q^{\alpha(J-m_\alpha)}|m_\alpha\rangle_\alpha,$$

where the sum is over all configurations for which $\sum_\alpha m_\alpha = M$ and the relationship between $\Delta > 1$ and $q \in (0, 1)$ is given by $\Delta = (q+q^{-1})/2$. A straightforward calculation shows a sharp transition in the magnetization from fully polarized down at the left to fully polarized up at the right. For this reason they are called kink ground states. In [7], Koma *et al* showed that there is a spectral gap above each of the ground states in this model for all values of J. Recently [8], we were able to prove the following theorem.

Theorem 1. *For spin values $J \geqslant \frac{3}{2}$, there exists a finite Δ_0 so that for all $\Delta > \Delta_0$, the first excited state of the restriction of $H_L^{\mathrm{k}}(\Delta^{-1})$ to any sector with fixed magnetization, are isolated eigenvalues that persist in the thermodynamic limit. This first excited state is a simple eigenvalue except when J is an integer > 1 and $M = 0 \bmod 2J$, in which case it is two-fold degenerate. As J increases, further isolated eigenvalues appear in the spectrum, which are also at most two-fold degenerate.*

In this paper, it was also proved that in certain values of spin and sector, for example $J = \frac{3}{2}$ and $M = 0$ both the ground and excited states are non-degenerate (simple eigenvalues). This is the qubit space we work with and our quantum gates will be unitaries on this space.

3. Quantum gates using quantum control

The problem of constructing quantum gates can be formulated as a problem in quantum control theory [15]. The goal is to steer the system using a small number of control parameters such that the unitary operator describing the quantum dynamics after a finite time T, has maximal overlap with a desired target unitary (the gate). From a control perspective these problems reduce to control of bilinear systems evolving on finite-dimensional Lie groups. This is an optimal control problem on a two-level system which has been studied widely with exact results known in some cases. For example, time optimal implementation of single and two-qubit quantum gates was studied [16] when the Lie algebra g of $su(2)$ ($su(4)$) can be decomposed as a Cartan pair $g = k \oplus p$ where k is the Lie subalgebra generated by the drift Hamiltonian and p is the Lie subalgebra generated by the control Hamiltonians. Finding the time optimal trajectories is reduced to finding geodesics on the coset space G/K (G and K being the Lie Groups corresponding to g and k). The problem of driving the evolution operator while minimizing an energy-type quadratic cost was studied in [17]. In this case the optimal solutions can be expressed as elliptic functions. The time optimal problem of population transfer problem of a two-level quantum system and bounded controls was studied in [18] and again explicit expressions for the optimal trajectories. In this paper, we follow a numerical gradient-based approach to optimal control [19, 20].

3.1. Single qubit gates

We consider the problem of time evolution of the one-dimensional XXZ chain under external controls. The equation of motion for the unitary evolution of the XXZ chain isolated from the

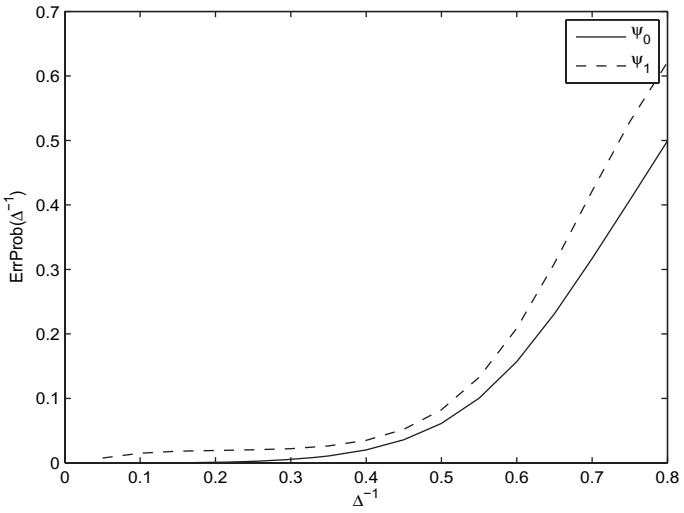

Figure 2. ErrProb, defined in (4), as a function of Δ^{-1}, calculated for the ground and first excited state ψ_0 and ψ_1, with $H^{\text{ext}} = S_0^3 S_1^3$. This quantity provides a measure of the escape rate out of the qubit subspace.

environment is given by Schrödinger's equation

$$\dot{U}(t) = -\mathrm{i}\Big(H_L^{\mathrm{k}}(\Delta^{-1}) + v(t)H^{\text{ext}}\Big)U, \quad U(0) = \mathbb{1}. \tag{2}$$

In control terminology $H_L^{\mathrm{k}}(\Delta^{-1})$ is the free or drift Hamiltonian and H^{ext} is the control Hamiltonian corresponding to the control field $v(t)$. We require that $\mathcal{D}$ is an invariant subspace of H^{ext}, so that the time evolution of the system 2 given by the unitary $U(t)$ starting from an initial state in $\mathcal{D}$ will be constrained to $\mathcal{D}$ at all future times. The induced evolution on $\mathcal{D}$ at any specified final time T will be the quantum gate on the qubit space $\mathcal{D}$ and is given by the 2×2 matrix

$$(U_{xxz})_{ij} := \langle \psi_i | U(T) | \psi_j \rangle, \quad i = 0, 1. \tag{3}$$

The control Hamiltonian we choose is the two-site operator $H^{\text{ext}} = S_0^3 S_1^3$. In practice for $S_0^3 S_1^3$ there is a very small error probability for states to move out of $\mathcal{D}$ and the matrix U_{xxz} is not exactly unitary. The matrix elements $\langle \psi_0 | H^{\text{ext}} | \psi_k \rangle$ and $\langle \psi_1 | H^{\text{ext}} | \psi_k \rangle$ $k \neq 0, 1$ are proportional to the transition probabilities to move from states ψ_0 and ψ_1 to other eigenstates of $H_L^{\mathrm{k}}(\Delta^{-1})$. We calculate the error probability to move out of the subspace $\mathcal{D}$ by the following estimates of these matrix elements

$$\text{ErrProb} = \|H^{\text{ext}}\psi_i\|^2 - |\langle \psi_0 | H^{\text{ext}} \psi_i \rangle|^2 - |\langle \psi_1 | H^{\text{ext}} \psi_i \rangle|^2, \tag{4}$$

for $i = 0, 1$. Figure 2 shows that the probabilities of transitioning out of the subspace $\mathcal{D}$ are extremely small for $\Delta^{-1} \leqslant 0.3$.

3.2. Implementing two-qubit gates

The idea for implementing two-qubit gates is to use two copies of the XXZ chain. The Hilbert space for two-qubit quantum computation is $\mathcal{D}_1 \otimes \mathcal{D}_2 \cong \mathbb{C}^4$, where $\mathcal{D}_1$ and $\mathcal{D}_2$ are the subspaces

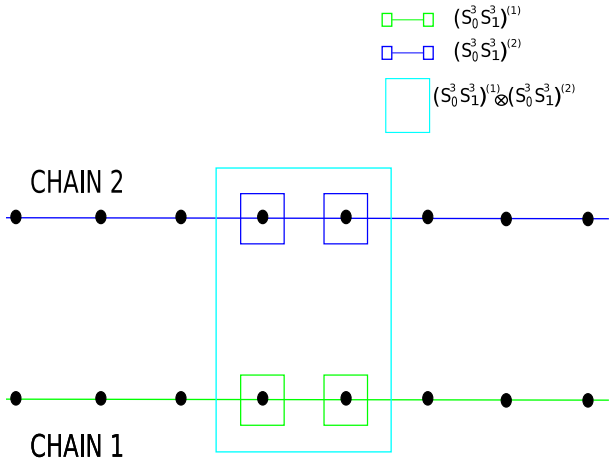

Figure 3. Configuration of two XXZ chains showing the localized controls required to implement the C-Not gate.

spanned by the ground state and the first excited state of the first chain and the second chain, respectively. The Hamiltonian of an uncoupled two chain system is given by

$$H_L^{\mathrm{k}}(\Delta^{-1})^{(1,2)} := H_L^{\mathrm{k}}(\Delta^{-1})^{(1)} + H_L^{\mathrm{k}}(\Delta^{-1})^{(2)}.$$

Here the notation $H_L^{\mathrm{k}}(\Delta^{-1})^{(1)}$ is to be interpreted as $\underbrace{H_L^{\mathrm{k}}(\Delta^{-1})}_{\text{chain 1}} \otimes (\underbrace{\mathbb{I}\otimes\cdots\otimes\mathbb{I}}_{\text{chain 2}})$ and $H_L^{\mathrm{k}}(\Delta^{-1})^{(2)}$ is to be interpreted as $(\underbrace{\mathbb{I}\otimes\cdots\otimes\mathbb{I}}_{\text{chain 1}}) \otimes \underbrace{H_L^{\mathrm{k}}(\Delta^{-1})}_{\text{chain 2}}$. The two-qubit space is spanned by the four vectors $\psi_{mn} := \psi_m \otimes \psi_n$ for $m, n = 0, 1$ which are eigenvectors of the above Hamiltonian. If we consider the control system

$$\dot{U} = -\mathrm{i}\Big(H_L^{\mathrm{k}}(\Delta^{-1})^{(1,2)} + v_1(t)(S_0^3S_1^3)^{(1)} + v_2(t)(S_0^3S_1^3)^{(2)}\Big)U, \tag{5}$$

with $U(0) = \mathbb{I}$, then by selectively turning on $v_1(t)$ and $v_2(t)$ for certain time periods, the above system is equivalent to the control system (2) on chains 1 and 2, respectively, during those time intervals. This can be used to generate single qubit gates on $\mathcal{D}_1$ and $\mathcal{D}_2$. Moreover, by simultaneously using $v_1(t)$ and $v_2(t)$ the local gates, i.e. gates of the kind $X_1 \otimes Y_2$ can be generated on $\mathcal{D}_1 \otimes \mathcal{D}_2$. To implement a two-qubit quantum computing scheme we need to also implement perfectly entangling gates, i.e. a gate that can take a product state to a maximally entangled state. It is known that single qubit gates and any perfectly entangling gate are universal for two-qubit quantum computing [21]. Clearly such a gate cannot be implemented by the control scheme (5) alone. In this paper, we choose to implement the C-Not gate, which is an example of a perfectly entangling gate. For this purpose we make use of an additional control namely $(S_0^3S_1^3)^{(1)} \otimes (S_0^3S_1^3)^{(2)}$.

We demonstrate the C-Not gate to high precision by using following control system

$$\dot{U} = -\mathrm{i}\Big(H_L^{\mathrm{k}}(\Delta^{-1})^{(1,2)} + v_1(t)(S_0^3S_1^3)^{(1)} + v_2(t)(S_0^3S_1^3)^{(2)} + v_3(t)(S_0^3S_1^3)^{(1)} \otimes (S_0^3S_1^3)^{(2)}\Big)U, \tag{6}$$

with $U(0) = \mathbb{I}$ by selectively turning on and off some or all of the control fields $v_1(t)$, $v_2(t)$ and $v_3(t)$ for specified time periods. Figure 3 shows a diagrammatic representation of the two-qubit

scheme. The C-Not gate is then given by the 4×4 matrix with elements

$$(\mathrm{C-Not}^{xxz})_{mn;rs} := \langle \psi_{mn}|U(T)|\psi_{rs}\rangle \; i = 0, 1.$$

3.3. Optimal control

We first solve the control problems (2) and (6) for the projected system on $\mathcal{D}$ for the single chain and $\mathcal{D}_1 \otimes \mathcal{D}_2$ for two chain system.

$$\dot{U}(t) = -\mathrm{i}\Big(H + \sum_k v_k(t) B_k\Big) U, \quad U(0) = \mathbb{1} \tag{7}$$

For the projected system on $\mathcal{D}$ the H and B_ks are given by the 2×2 matrices

$$\begin{aligned} H_{ij} &= \langle \psi_i | H_L^{\mathrm{k}}(\Delta^{-1}) | \psi_j \rangle, \\ (B_1)_{ij} &= \langle \psi_i | H_L^{\mathrm{k}}(\Delta^{-1}) | \psi_j \rangle, \quad i, j = 0, 1, \end{aligned} \tag{8}$$

whereas the projected system on $\mathcal{D}_1 \otimes \mathcal{D}_2$ the control problem involves 4×4 matrices

$$\begin{aligned} H_{mn;rs} &= \langle \psi_{mn} | H_L^{\mathrm{k}}(\Delta^{-1})^{(1,2)} | \psi_{rs} \rangle, \\ (B_1)_{mn;rs} &= \langle \psi_{mn} | (S_0^3 S_1^3)^{(1)} | \psi_{rs} \rangle, \\ (B_2)_{mn;rs} &= \langle \psi_{mn} | (S_0^3 S_1^3)^{(2)} | \psi_{rs} \rangle, \\ (B_3)_{mn;rs} &= \langle \psi_{mn} | (S_0^3 S_1^3)^{(1)} \otimes (S_0^3 S_1^3)^{(2)} | \psi_{rs} \rangle, \end{aligned} \tag{9}$$

where $m, n, r, s = 0, 1$. The overlap between a desired unitary gate U_f and the solution of (6) at time T, $U(T)$, is measured as the difference in the norm square $\| U_f - U(T) \|^2$, and the norm is defined in terms of the standard inner product $\langle V | W \rangle := \mathrm{Tr}(V^\dagger W)$. The norm can be written as

$$\|U_f - U(T)\|^2 = \|U_f\|^2 - 2\mathrm{Re}\langle U_f | U(T)\rangle + \|U(T)\|^2$$

and hence minimizing this norm is equivalent to maximizing

$$\Phi := \mathrm{Re}\langle U_f | U(T)\rangle = \mathrm{Tr}(U_f^\dagger U(T)). \tag{10}$$

We define the gate fidelity as

$$\mathcal{F}_{\mathrm{Gate}} := \frac{|\mathrm{Tr}(U_f^\dagger U(T))|}{\mathrm{Tr}(\mathbb{1})}. \tag{11}$$

To select the optimal control fields $v_i(t)$ we use the numerical gradient ascent approach described in many books on control theory. This approach was applied to the quantum setting in [20]. We start with the necessary conditions for optimality called the Pontryagin maximum principle which is a generalization of the Euler–Lagrange equations from calculus of variations. In the problems with costs of type (10) and no *a priori* bound on controls, Pontryagin's maximum principle takes the following form.

Theorem 2. *(Pontryagin maximum principle [20, 22]). If $v_i(t)$s are optimal controls of the system (6) and $U(t)$ the corresponding trajectory solution, then there exists a nonzero operator valued Lagrange multiplier λ which is the solution of the adjoint equations*

$$\dot{\lambda}(t) = -\mathrm{i}H(t)\lambda(t), \qquad \text{with terminal condition,}$$

$$\lambda'(T) = -\frac{\partial \Phi(T)}{\partial U(T)} = -U_f,$$

and a scalar valued Hamiltonian function $h(U(t), v_i(t)) := \mathrm{Re}\,\mathrm{Tr}(-\mathrm{i}\lambda'(t)H(t)U(t))$ such that, for every $\tau \in (0, T]$ we have

$$\frac{\partial h(U)}{\partial v_i} = \mathrm{Im}\,\mathrm{Tr}(\lambda'(t)B_iU(t)) = 0. \tag{12}$$

The algorithm to find the optimal controls is as follows:

(i) A suitable gate time T is chosen and discretized in N equal steps of duration $\Delta t = \frac{T}{N}$. The initial control $v_i^{(0)}(t_k)$ for all the discretized time intervals is based on a guess or at random.

(ii) For these piecewise constant controls, from $U(0) = \mathbb{I}$ and $\lambda(T) = -U_f$, compute the forward and backward propagation respectively as follows

$$U^{(r)}(t_k) = F^{(r)}(t_k)F^{(r)}(t_{k-1}) \ldots F^{(r)}(t_1), \tag{13}$$

$$\lambda^{(r)}(t_k) = F^{(r)}(t_k)F^{(r)}(t_{k+1}) \ldots F^{(r)}(t_N)\lambda(T), \tag{14}$$

for all $t_1, \ldots, t_N$ and where r is an iteration number of the algorithm initially set to 0 and

$$F^{(r)}(t_k) = \exp\left\{-\mathrm{i}\Delta t\left(H + \sum_i v_i^{(r)}(t_k)B_i\right)\right\}.$$

(iii) Substitute the equations (13) and (14) into equation (12) to evaluate the gradient, and then update the controls as

$$v_i^{(r+1)}(t_k) = v_i^{(r)}(t_k) + \tau\frac{\partial h(U(t_k), v_i(t_k))}{\partial v_i},$$

where τ is a small step size.

(iv) if $\mathcal{F}_{\mathrm{Gate}} < \gamma$ (γ being the level of accuracy) then done, otherwise go to step (2) for the next iteration with the updated controls.

Having solved the control problem on the projected systems to get the optimal controls $v_1(t)$, $v_2(t)$ and $v_3(t)$ we would like to apply them to a large system and see their effects on the projected system. However simulating even a moderately sized spin chain is hard because of the exponentially growing dimension of the Hilbert space. In the next section we describe an algorithm by which we are able to simulate the XXZ chain of 50 sites.

4. DMRG simulations for quantum gates

To see the effect of the evolution of the XXZ chain with external magnetic controls we numerically simulate the XXZ chain using the DMRG algorithm. The dynamics of the interfaces of the XXZ chain using DMRG was studied recently in [23]. The standard DMRG algorithm is a numerical algorithm originally developed by White [24] that has worked successfully in providing very accurate results for ground state energies and correlation functions in strongly correlated systems. Modifications to this method [25, 26] allow to address the physics of time-dependent and out of equilibrium systems. The crux of the DMRG algorithm is a decimation procedure that chooses the physically most relevant states to describe the target states. It is now known that DMRG works well because the ground states of non-critical quantum chains like the XXZ chain are only slightly entangled, i.e. they obey an area law of entanglement that says that the entanglement between a distinguished block of the chain and the rest of the chain is bounded by the boundary area of the block. In fact the DMRG procedure is a variational ansatz over states known as Matrix product states (MPS) [27]. The standard DMRG procedure and its connection with MPS and entanglement is described in detail in [28]. For a single XXZ chain our target states are the ground state ψ_0 and first excited state ψ_1 restricted to a sector of magnetization. We use the standard DMRG procedure with the adaptation that we grow the chain while restricting the blocks to the sector of zero magnetization using the symmetry of the Hamiltonian (see [23]).

For the two-qubit gates we convert the two chain system to a one dimensional spin chain by a spin ladder construction.

$$\begin{array}{ccccccccc} \mathcal{H}^{(1)}_{-L+1} & & \otimes & & \mathcal{H}^{(1)}_{-L+2} & & \otimes \ \ldots \ \otimes & & \mathcal{H}^{(1)}_{L} \\ \otimes & & & & \otimes & & & & \otimes \end{array} = \mathcal{H}^{(1)}_{[-L+1,L]},$$

$$\mathcal{H}^{(2)}_{-L+1} \otimes \mathcal{H}^{(2)}_{-L+2} \otimes \ \ldots \ \otimes \mathcal{H}^{(2)}_{L} = \mathcal{H}^{(2)}_{[-L+1,L]}.$$

The single site Hilbert space for the DMRG is the rung composed of $\mathcal{H}^{(1)}_{\alpha} \otimes \mathcal{H}^{(2)}_{\alpha}$ for $\alpha \in [-L+1 \ldots L]$. On this site we define the local operators

$$S^{i(1)}_{\alpha} = S^{i}_{\alpha} \otimes \mathbb{I}_{\alpha}, \quad S^{i(2)}_{\alpha} = \mathbb{I}_{\alpha} \otimes S^{i}_{\alpha}, \quad \text{for } i = 1, 2, 3.$$

We can then write the Hamiltonian of this single chain using the above construction

$$H^{\mathrm{k}}_{L}(\Delta^{-1})^{(1,2)} := \sum_{\alpha=-L+1}^{L-1} h^{(1)}_{\alpha,\alpha+1}(\Delta^{-1}) + h^{(2)}_{\alpha,\alpha+1}(\Delta^{-1}), \tag{15}$$

$$h^{(k)}_{\alpha,\alpha+1}(\Delta^{-1}) = J^2 - S^{3(k)}_{\alpha} S^{3(k)}_{\alpha+1} - \Delta^{-1}(S^{1(k)}_{\alpha} S^{1(k)}_{\alpha+1} + S^{2(k)}_{\alpha} S^{2(k)}_{\alpha+1}) + J\sqrt{1-\Delta^{-2}}(S^{3(k)}_{\alpha} - S^{3(k)}_{\alpha+1}), \tag{16}$$

for $k = 1, 2$. We carry out the DMRG procedure as described in the algorithm with the Hamiltonian $H^{\mathrm{k}}_{L}(\Delta^{-1})^{(1,2)}$ but we ensure that we keep both the chains in the magnetization sector 0 by simultaneously diagonalizing $H^{\mathrm{k}}_{L}(\Delta^{-1})^{(1,2)}$ with the total magnetization operators

$$S^{(k)}_{\mathrm{tot}} = \sum_{\alpha=-L+1}^{L} S^{3(k)}_{\alpha}, \quad \text{for } k = 1, 2.$$

The target states $\psi_0 \otimes \psi_0$, $\psi_0 \otimes \psi_1$, $\psi_1 \otimes \psi_0$, $\psi_1 \otimes \psi_1$ are the simultaneous eigenvectors of the these operators and form the computational basis $|00\rangle$, $|01\rangle$, $|10\rangle$ and $|11\rangle$ for two-qubit quantum computation.

To compute the time evolution of the chain under the controlled evolution by the external fields we use the time-dependent DMRG procedure. The idea is that a two-site operator can be applied to a DMRG state most effectively by expressing the state in the basis where the left block has length $x-1$ so the two middle sites that are untruncated are the sites where the operator is acting. We can write the time evolution in the Trotter decomposition

$$e^{-iH\delta} \cong e^{-(i/2)h_{-L+1,-L+2}} e^{-(i/2)h_{-L+2,-L+3}} \cdots e^{-(i/2)h_{L-2,L-1}} e^{-(i/2)h_{L-1,L}} + O(\delta^3). \tag{17}$$

To apply $e^{-iH\delta}$ to the ground and excited states in the basis with the center sites all the way to the left we apply $e^{-(i/2)h_{-L+1,-L+2}}$. After shifting one site to the right we apply $e^{-(i/2)h_{-L+2,-L+3}}$ etc. Since all our controls are two site controls at the center, only the interaction $h_{0,1}$ is time-dependent. In the adaptive time-dependent methods the Hilbert space is continuously modified as time progresses by carrying out reduced basis transformations on the evolved state. In our case since the gates are obtained in a relatively short period of time our Hilbert space remains unchanged resembling the static DMRG methods.

5. Results

In this section, we present numerical results of the construction of quantum gates using the spin-$\frac{3}{2}$ XXZ spin chain. Our results are for the universal set of single qubit gates consisting of the Not (X), Hadamard (H), Pi-8 (T) and Phase (S) gates and the two-qubit C-Not gate. All results are obtained using the DMRG algorithm and the optimal control methods described in the previous sections. The steps carried out to obtain the single qubit gates are as follows:

(i) We use ground state DMRG of the XXZ chain to obtain the lowest eigenvectors ψ_0 and ψ_1 of $H_L^k(\Delta^{-1})$ in the sector corresponding to $M = 0$.

(ii) We obtain the projected 2×2 control system of equation (7) with matrices H and B_1 with matrix elements given by (8). For a target gate U_f and a suitable final time T we find the optimal control $v_1(t)$ on this 2×2 system using the technique described in section 3.3.

(iii) Finally we apply the time-dependent DMRG procedure of section 4 to the chain of (2) for a specified time T starting from ψ_0 and ψ_1 and using the $v_1(t)$ found in step 2 to get the time evolved states $\psi_0(T) = U(T)\psi_0$ and $\psi_1(T) = U(T)\psi_1$. We compute the induced evolution on the subspace $\mathcal{D}$ to obtain the gate U_{xxz} given by the matrix elements $\langle\psi_i|\psi_j(T)\rangle$ for $i, j = 0, 1$ and compare the overlap with U_f using equation (11).

Our desired single-qubit target gates are given by the unitaries.

$$X = \begin{pmatrix} 0 & i \\ i & 0 \end{pmatrix}, \qquad H = \frac{1}{\sqrt{2}} \begin{pmatrix} i & i \\ i & -i \end{pmatrix},$$

$$S = \begin{pmatrix} e^{-i\pi/4} & 0 \\ 0 & e^{-i\pi/4} \end{pmatrix}, \quad T = \begin{pmatrix} e^{-i\pi/8} & 0 \\ 0 & e^{-i\pi/8} \end{pmatrix}.$$

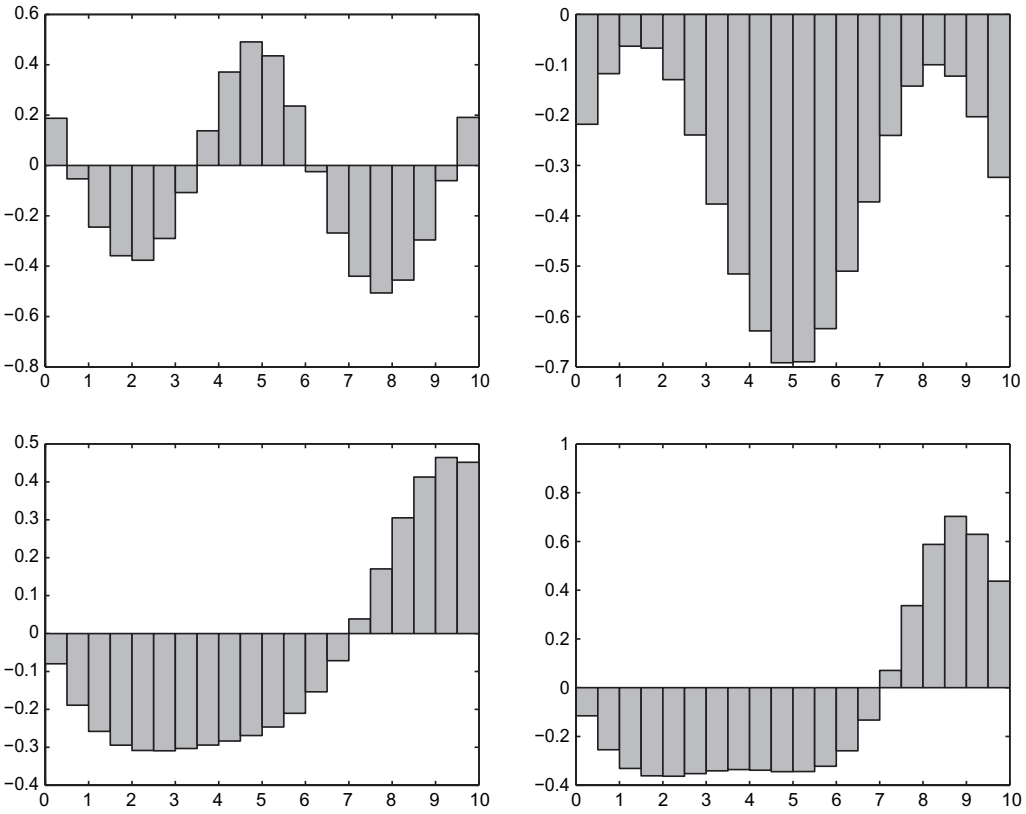

Figure 4. (Clockwise) The controls for Not, Hadamard, Pi-8 and Phase gates plotted versus time discretized for time steps of $\Delta t = 0.5$.

Note that the X and H gates have a extra factor i with respect to the conventional definition. This turned out to be convenient for us but is otherwise not important. The gates obtained using the XXZ chain and their fidelities are as follows. The optimal controls $v_1(t)$ used to get the gate results are shown in figure 4 and table 1.

$$X_{xxz} = \begin{pmatrix} 0.0016 - 0.0011i & 0.0033 + 0.9997i \\ -0.0017 + 0.9997i & 0.0017 + 0.0011i \end{pmatrix}, \qquad \mathcal{F}_X = 0.9997,$$

$$H_{xxz} = \begin{pmatrix} -0.0027 + 0.7081i & 0.0011 + 0.7053i \\ -0.0016 + 0.7052i & -0.0022 - 0.7085i \end{pmatrix}, \qquad \mathcal{F}_H = 0.9995,$$

$$T_{xxz} = \begin{pmatrix} 0.9221 - 0.3859i & -0.0037 + 0.0038i \\ 0.0037 + 0.0038i & 0.9216 + 0.3871i \end{pmatrix}, \qquad \mathcal{F}_T = 0.9995,$$

$$S_{xxz} = \begin{pmatrix} 0.7043 - 0.7095i & -0.0046 + 0.0015i \\ 0.0045 + 0.0016i & 0.7017 + 0.7121i \end{pmatrix}, \qquad \mathcal{F}_S = 0.9997.$$

Table 1. Numerical simulation of the construction of the Not, Pi-8, Hadamard and Phase gates. Results are obtained using DMRG and time-dependent DMRG for a spin-$\frac{3}{2}$ chain of $L = 50$ sites and at $\Delta^{-1} = 0.3$ in the sector corresponding to $M = 0$. The table shows the values of the control field $v_1(t)$ with gate time $T = 10$ discretized with $\Delta t = 0.5$.

Not (X)	Hadamard (H)	Pi-8 (T)	Phase (S)
0.1874	−0.2182	−0.1152	−0.0797
−0.0533	−0.1176	−0.2544	−0.1889
−0.2447	−0.0631	−0.3310	−0.2579
−0.3587	−0.0670	−0.3613	−0.2945
−0.3764	−0.1296	−0.3632	−0.3085
−0.2901	−0.2396	−0.3524	−0.3091
−0.1075	−0.3766	−0.3410	−0.3031
0.1376	−0.5154	−0.3358	−0.2943
0.3712	−0.6286	−0.3383	−0.2836
0.4908	−0.6917	−0.3443	−0.2691
0.4355	−0.6899	−0.3441	−0.2466
0.2359	−0.6241	−0.3222	−0.2103
−0.0246	−0.5099	−0.2590	−0.1538
−0.2681	−0.3723	−0.1328	−0.0715
−0.4399	−0.2404	0.0709	0.0386
−0.5065	−0.1424	0.3368	0.1704
−0.4553	−0.1001	0.5877	0.3053
−0.2959	−0.1225	0.7029	0.4128
−0.0605	−0.2033	0.6294	0.4642
0.1909	−0.3236	0.4374	0.4516

For the C-Not gate the procedure described earlier is only slightly modified. We use the ground state DMRG of a one-dimensional chain built from the spin ladder described in section 4 to get four eigenvectors ψ_{mn} for $m, n = 0, 1$. The optimal control procedure is applied to the 4×4 control system (7) with H, B_1, B_2, B_3 given by equations (9) to find the controls $v_1(t)$, $v_2(t)$ and $v_3(t)$. The time-dependent DMRG procedure is applied to the chain of equation (6) for time T with the controls $v_1(t)$, $v_2(t)$ and $v_3(t)$ to get the time-evolved states $\psi_{mn}(T) = U(T)\psi_{mn}$. The induced evolution on the subspace $\mathcal{D}_1 \otimes \mathcal{D}_2$ gives the $\mathrm{C-Not}_{xxz}$ gate with matrix elements $\langle \psi_{mn} | \psi_{rs}(T) \rangle$. Table 2 shows the optimal controls $v_1(t)$, $v_2(t)$ and $v_3(t)$ used to obtain the C-not gate. The gate obtained using the XXZ chain and gate fidelity is as follows:

$$\mathrm{C-Not} = \begin{pmatrix} 1 & 0 & 0 & 0 \\ 0 & 1 & 0 & 0 \\ 0 & 0 & 0 & 1 \\ 0 & 0 & 1 & 0 \end{pmatrix},$$

Table 2. The C-Not gate controls using two spin-$\frac{3}{2}$ XXZ-chains of length $L = 50$ at $\Delta^{-1} = 0.25$ and $M = 0$ for both the chains. The gate time $T = 3.5$ is discretized into $N = 20$ time steps. The table shows the values for the three control fields v_1, v_2 and v_3 that are constant during any one of the time intervals.

$v_1(t)$	$v_2(t)$	$v_3(t)$
−0.4040	0.3953	0.0540
2.4494	0.2588	0.0501
3.7163	0.1886	−0.1314
3.0455	0.1766	−0.2677
1.6565	0.2185	−0.0872
0.5583	0.3085	0.1455
−0.1036	0.4206	0.2346
−0.5117	0.5196	0.1648
−0.8215	0.5716	−0.0282
−1.0083	0.5578	−0.3599
−0.8630	0.4926	−0.9102
−0.3774	0.3612	−1.4955
−0.0810	0.0978	−1.4905
−0.0940	−0.1214	−0.9196
−0.0881	−0.1138	−0.3217
−0.0408	0.0794	0.0922
−0.1805	0.3399	0.3374
−0.8094	0.5868	0.4146
−2.2183	0.8522	0.2021
−4.2425	1.2694	−0.4760

$$\mathrm{C-Not}_{\mathrm{xxz}} =$$

$$\begin{pmatrix} 0.9959+0.0001i & -0.0015+0.0006i & 0.0003-0.0003i & -0.0010-0.0001i \\ -0.0014-0.0010i & 0.9939-0.0003i & 0.0015+0.0000i & -0.0005+0.0005i \\ 0.0013-0.0001i & 0.0004+0.0003i & 0.0004-0.0003i & 0.9945-0.0008i \\ -0.0003-0.0003i & -0.0013+0.0002i & 0.9954-0.0004i & 0.0003+0.0003i \end{pmatrix},$$

$$\mathcal{F}_{\mathrm{C-Not}} = 0.9949.$$

Acknowledgments

Based upon work supported in part by the National Science Foundation under grant nos DMS-0605342 and DMS-0757581. JM also received support from NSF Vigre grant no. DMS-0636297.

References

[1] Cirac J and Zoller P 1995 *Phys. Rev. Lett.* **74** 4091
[2] Monroe C, Meekhof D, King B, Itano W and Wineland D 1995 *Phys. Rev. Lett.* **75** 4714
[3] Mooij J, Orlando T, Levitov L, Tian L, van der Wal C and Lloyd S 1999 *Science* **285** 1036
[4] Chuang I, Vandersypen L, Zhou X, Leung D and Lloyd S 1998 *Nature* **393** 143
[5] Loss D and DiVincenzo D 1998 *Phys. Rev.* A **57** 120
[6] Pasquier V and Saleur H 1990 *Nucl. Phys.* B **330** 523
[7] Koma T, Nachtergaele B and Starr S 2001 *Adv. Theor. Math. Phys.* **5** 1047
[8] Mulherkar J, Nachtergaele B, Sims R and Starr S 2008 *J. Stat. Mech.* P01016
[9] Barenco A *et al* 1995 *Phys. Rev.* A **52** 3457
[10] Alcaraz F, Salinas S and Wreszinski W 1995 *Phys. Rev. Lett.* **75** 930
[11] Gottstein C and Werner R 1995 arXiv:cond-mat/9501123
[12] Matsui T 1996 *Lett. Math. Phys.* **37** 397
[13] Koma T and Nachtergaele B 1998 *Adv. Theor. Math. Phys.* **2** 533
[14] Nachtergaele B, Spitzer W and Starr S 2003 *Contemp. Math. Am. Math. Soc.* **327** 251
[15] Mabuchi H and Khaneja N 2005 *Int. J. Robust. Nonlinear Control* **15** 647
[16] Khaneja N, Brockett R and Glaser S 2001 *Phys. Rev.* A **63** 032308
[17] D'Alessandro D and Dahleh M 2001 *IEEE Trans. Autom. Control* **46** 866
[18] Boscain U and Mason P 2005 *Proc. 44th IEEE Conf. on Decision and Control and the European Control Conf.*
[19] D'Alessandro D 2008 *Introduction to Quantum Control Dynamics (CRC Applied Mathematics and Nonlinear Science Series)* (London: Chapman and Hall)
[20] Khaneja N, Reiss T, Kehlet C, Schulte-Herbruggen T and Glasser S 2005 *J. Magn. Reson.* **172** 296
[21] Zhang J, Vala J, Sastry S and Whaley K 2003 *Phys. Rev. Lett.* **91** 027903
[22] Bruß D and Leuchs G 2007 *Lectures on Quantum Information* (New York: Wiley-VCH)
[23] Michoel T, Nachtergaele B and Spitzer W 2008 *J. Phys. A: Math. Theor.* **41** 492001
[24] White S 1993 *Phys. Rev.* B **48** 10345
[25] Vidal G 2004 *Phys. Rev. Lett.* **93** 040502
[26] White S and Feiguin A 2004 *Phys. Rev. Lett.* **93** 076401
[27] Fannes M, Nachtergaele B and Werner R 1992 *Commun. Math. Phys.* **144** 443
[28] Schollwock U 2005 *Rev. Mod. Phys.* **77** 259